In situ oxidation of ultrathin silver films on Ni(111)

A. Meyer
J. I. Flege
S. D. Senanayake
B. Kaemena
R. E. Rettew
F. M. Alamgir
J. Falta

Oxidation of silver films of one- and two-monolayer thicknesses on the Ni(111) surface was investigated by low-energy electron microscopy at temperatures of 500 and 600 K. Additionally, intensity–voltage curves were measured in situ during oxidation to reveal the local film structure on a nanometer scale. At both temperatures, we find that exposure to molecular oxygen leads to the destabilization of the Ag film with subsequent relocation of the silver atoms to small few-layer-thick silver patches and concurrent evolution of NiO(111) regions. Subsequent exposure of the oxidized surface to ethylene initiates the transformation of bilayer islands back into monolayer islands, demonstrating at least partial reversibility of the silver relocation process at 600 K.

Introduction

The development of novel materials for technical purposes, for example, in catalytic processes, has become of great interest in the last decade. In particular, for chemical reactions such as oxidation processes, the electronic and geometrical properties of the surface play an important role in the functionality of the system. Therefore, the elements in the transition-metal series are the preferred candidates as active components because of their particular electronic structure resulting from the partially occupied d-band in the valence region [1, 2]. The combination of these transition metals with other metallic elements (e.g., noble metals) results in materials with tunable chemical and electronic properties by intentional electronic and structural modification of the near-surface region. One possible realization of such a multicomponent system is the growth of ultrathin films of a suitable element on a transition metal. In this respect, well-defined silver films on Ni(111) may be regarded as a model system because the two metals grow in the face-centered cubic structure and are virtually immiscible [3], allowing for the preparation of Ag(111) overlayers with a sharp interface under ultrahigh-vacuum (UHV) conditions [4, 5].

While the growth and reaction behavior of the bulk materials Ag(111) and Ni(111) during oxidation are fairly well understood, the reaction characteristics of the bimetallic system, here ultrathin silver films on Ni(111), with oxygen have not been investigated yet but can be expected to substantially differ from the bulk properties of the individual compounds. Oxidation of a Ag(111) crystal, for instance, leads to the formation of an ordered p(4 × 4) reconstruction around 500 K [6, 7]. The dissociative sticking probability for the adsorption of molecular oxygen on Ag(111) at 490 K is in the 10^{-6} range [8]. In contrast, oxygen exposure of Ni(111) causes a p(2 × 2) reconstruction [9] at doses less than 10 Langmuir ($1\ \mathrm{L} = 10^{-6}$ torr/s), whereas a higher dose at 300 K gives rise to the growth of ultrathin NiO(111) films [10]. The sticking coefficient of oxygen on Ni(111) at temperatures around 450 K is in the range of 10^{-2} [11], i.e., about four orders of magnitude higher than on Ag(111).

Low-energy electron microscopy (LEEM) is a technique that allows the investigation of surface processes during growth or oxidation on a length scale of a few nanometers in real time. In this paper, we present an *in situ* LEEM study of the oxidation of the bimetallic Ag/Ni surface. By determining the dependence of the electron reflectivity on the kinetic electron energy, which is generally known as LEEM intensity–voltage $[I(V)]$ curves, we were able to probe the local atomic structure and follow its modification during the oxidation reaction, an approach that we have already successfully applied to unravel oxidation-induced changes and subsequent catalytic reactions over single-crystal transition-metal surfaces [12, 13]. We show that oxygen exposure induces the formation of few-nanometer-sized silver-free nickel oxide grains concurrent with layer-dependent thickening of the silver islands. Finally, we demonstrate the partial reversibility of

Digital Object Identifier: 10.1147/JRD.2011.2157262

0018-8646/11/$5.00 © 2011 IBM

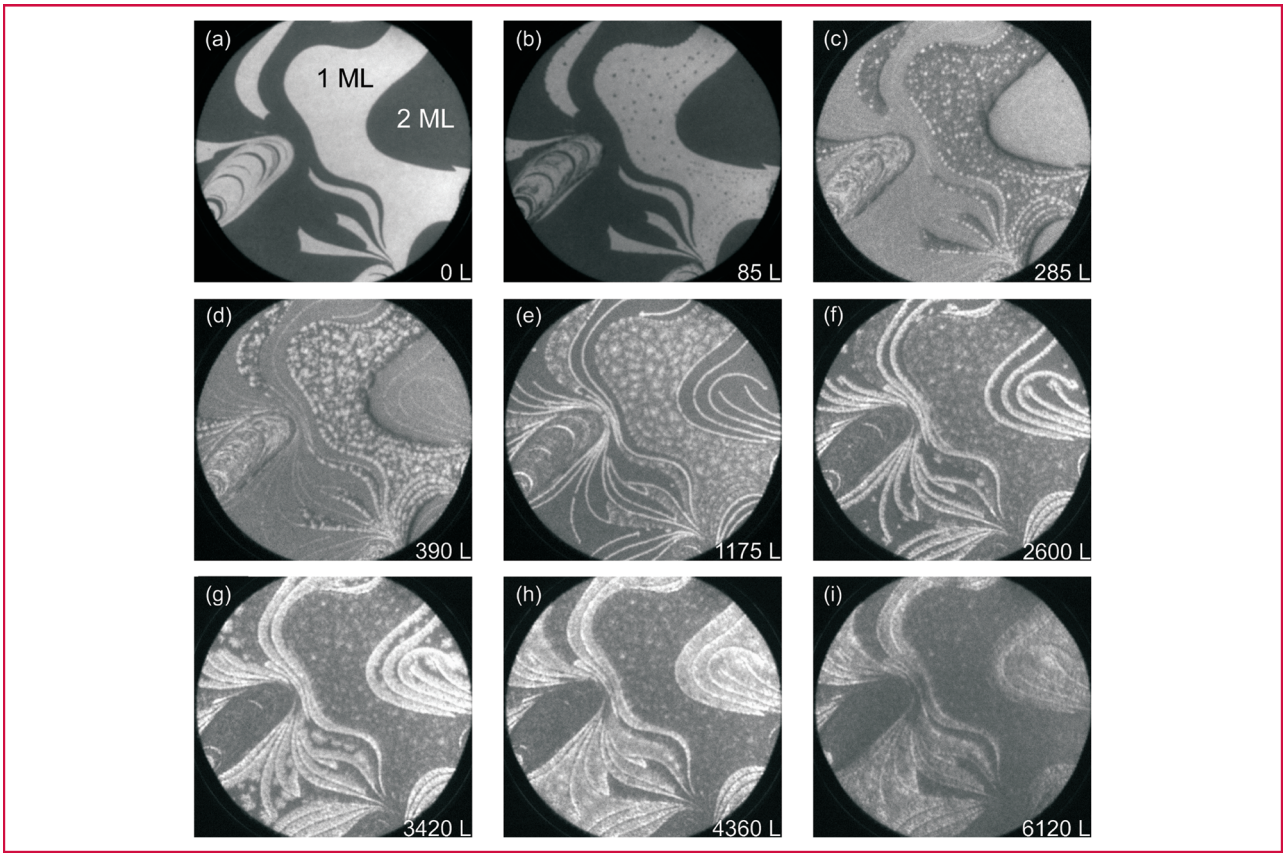

Figure 1

LEEM images of the reaction of the Ag-covered Ni(111) surface at 500 K with 6,120 L of molecular oxygen. Images have been taken at 2.7-eV electron energy and a 15-μm field of view. Oxidation starts on the one-monolayer silver film after 85 L of oxygen, whereas the two-monolayer-thick films become oxidized after 1,175 L.

the Ag dewetting process by dosing ethylene, which reduces the previously grown nickel oxide.

Experimental details

The measurements have been performed in a commercial Elmitec spectroscopic photoemission low-energy electron microscope at the beamline U5UA of the National Synchrotron Light Source at Brookhaven National Laboratory, Upton, NY, New York, United States [14]. Aside from the usage of low-energy electrons, the installation at the vacuum-ultraviolet storage ring and an energy filter also allow *in situ* microscopy with photoexcited electrons of a selected kinetic energy value. The UHV system contains a sputter gun for crystal cleaning purposes.

The sample used in this paper was a polished Ni(111) crystal with an orientation better than 0.1°. Before we started the experiments, the crystal was treated by several cycles of sputtering by Ar^+ ions at 0.5-keV kinetic energy and 5.0×10^{-5} torr Ar background pressure followed by annealing at 1,050 K, a cleaning procedure whose effectiveness has already been demonstrated [4]. Subsequent short flashes to 1,300 K gave rise to flattening of the surface. High-purity silver (99.9999%, Johnson Mathey Compound Company) was evaporated from a resistively heated crucible (Knudsen cell) equipped with a manual shutter and a quartz oscillator for flux control and water cooling.

After the sample cleaning procedure, the silver films were deposited on the Ni(111) crystal at sample temperatures of 750 K up to a coverage between one and two monolayers (MLs) (see **Figure 1**). The Ag coverage was controlled by LEEM images and LEEM-$I(V)$ fingerprints, which are already known from previous work [4], during evaporation. The low-energy electron diffraction (LEED) pattern of the Ag-covered surface showed the characteristic $\sqrt{52} \times \sqrt{52}$ R13.9° reconstruction [15].

Results

In this paper, we present our results on the oxidation behavior of this surface at temperatures of 500 and 600 K. At these temperatures, oxide layers form on both Ni(111) and Ag(111).

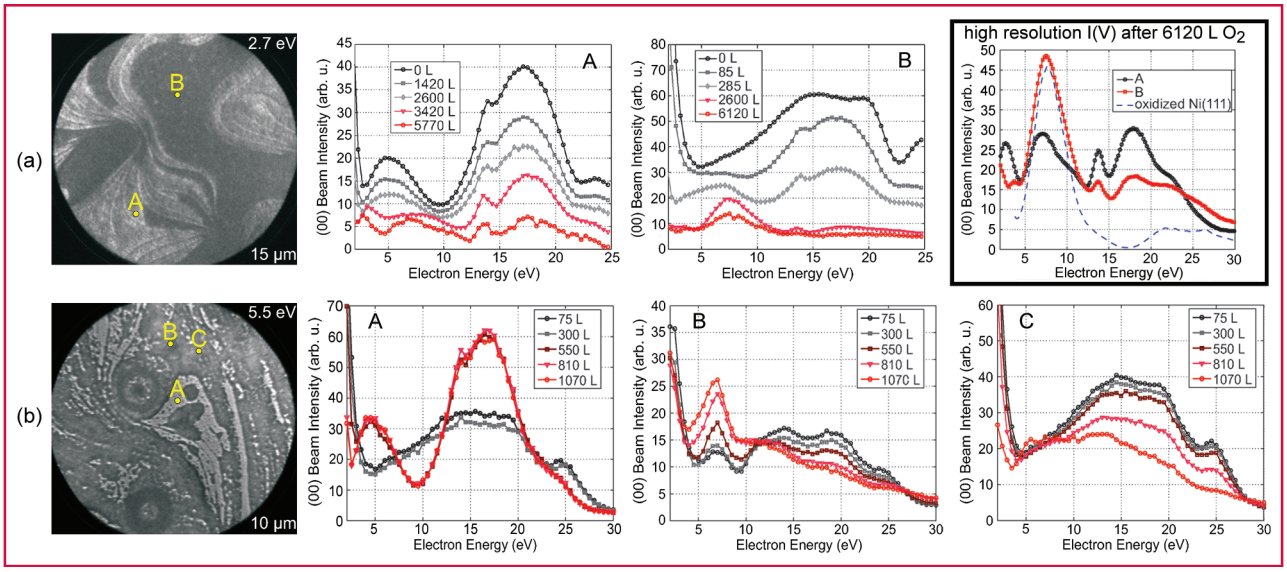

Figure 2

LEEM-$I(V)$ characteristics for typical regions of interest acquired during oxidation of the Ag/Ni(111) surface at (a) 500 K and (b) 600 K. The LEEM images show a field of view of (a) 15 and (b) 10 μm, respectively. (arb. u.: arbitrary units.)

Oxidation at 500 K

At a sample temperature of 500 K, a total amount of 6,120-L oxygen at a pressure of 2×10^{-6} torr has been dosed onto the bare Ag/Ni(111) surface [see Figure 1(a)–1(i)]. Here, the region covered by one-ML silver appears to be bright, and the two-ML Ag film appears dark. An oxygen dose of 85 L leads to the formation of small patches in the region of the one-ML silver film, first decorating the step edges and domain boundaries. The change in contrast between Figures 1(b) and 1(c) is related to a change in the $I(V)$ curves [see **Figure 2(a)**] in the observed surface area. Up to 1,175 L [see Figure 1(e)], the small patches on the one-ML film spread and gradually fill the whole first ML of Ag, whereas the two-ML silver film seems to be inert to oxygen except for a reaction at step edges. However, prolonged exposure up to 6,120 L does cause a change in reflectivity also for the Ag double layer, indicating a delayed reaction of the oxygen molecules starting from steps and defects [see Figure 1(f)–1(i)]. In a later section, the local changes in reflectivity are analyzed in terms of the local atomic structure by virtue of $I(V)$ curves taken during O_2 exposure.

Oxidation at 600 K

The clean Ag/Ni(111) surface for oxidation at 600 K is shown in **Figure 3(a)**. In this LEEM image, three different regions are visible. For the most part, the surface is covered by one ML of silver, whereas the smaller regions are covered by a double layer, but in contrast to the previous sample, there are still some areas where no closed silver film could be

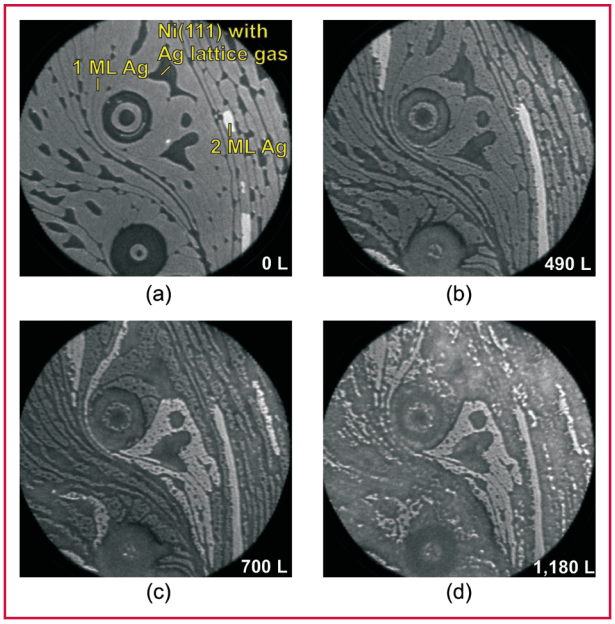

Figure 3

Oxidation of the Ni(111) surface with regions of one-ML silver coverage (gray), two-ML coverage (bright), and bare substrate (dark) after growth at 600 K. The LEEM images were taken at 5.5-eV electron energy and a 10-μm field of view during exposure up to 1,180 L of molecular oxygen.

obtained. After 490 L of oxygen dose at 7×10^{-7} torr, an intriguing phenomenon is observed: The two-ML silver islands appear to have grown along the step edges [see **Figure 3(b)**]. This process is found to proceed with increasing oxygen dose [see **Figure 3(d)** for a dose of 1,180 L]. In **Figure 3(c)**, a weak change in contrast can be also seen for the seemingly bare exposed Ni(111) areas. Moreover, the previously smooth ML silver film increasingly becomes more rugged and exhibits irregular island shapes.

Based on the contrast changes observed in the presented LEEM sequences recorded at fixed electron energy alone, unambiguous conclusions on the underlying atomic-scale processes and structural modifications cannot be drawn without further information. Therefore, in the following, we utilize the dynamic LEEM-$I(V)$ technique to perform a time-resolved analysis of the nanoscale atomic surface structure.

In situ local LEEM-$I(V)$ spectra taken at 500 and 600 K

The LEEM image and the corresponding $I(V)$ curves of oxidation at 500 K are presented in Figure 2(a). Before the oxygen dose, the local $I(V)$ curve at point "A" shows the fingerprint of a two-ML-thick silver film on Ni(111), whereas point "B" is identified as a one-ML silver film based on previous investigations [4]. Exposure to oxygen results in a change in the $I(V)$ characteristics with time. The local $I(V)$ curves of both points develop a new and common distinct feature at 7.5 eV after oxidation with 6,120 L of O_2. This peak is very dominant for surfaces covered with one ML of silver, but it also shows up after sufficient exposure (6,120 L) for double-layer films, whose $I(V)$ curves exhibit peaks at very similar positions aside from a small energy difference of the peaks at very low energy values [see the high-resolution $I(V)$ curve in Figure 2(a)].

The local $I(V)$ spectra taken at different points of the surface prepared at 600 K are shown in **Figure 2(b)**. Before starting the oxygen exposure, the $I(V)$ curves at points "A" and "C" indicate a silver film of one ML on Ni(111). In the region of point "B," the first silver layer is not closed; therefore, the $I(V)$ curve shows, in essence, the characteristics of the bare Ni(111) surface, including dispersed silver adatoms (also termed "lattice gas" in the literature), whose presence was previously shown [4] and the implications of which are described below. Integral exposures of 1,070 L of oxygen result in a change in the electron reflectivity at points "A" and "B," whereas the local energy-dependent intensity in point "C" is mostly unaffected.

Discussion

In the case of oxidation at 500 K, the surface consists of a mixture of regions covered by one- and two-ML silver before oxidation. A small oxygen dose of 85 L already causes a change in reflectivity for the one-ML silver film [see region "B" in Figure 2(a)]. Further oxidation up to 285 L leads to an $I(V)$ curve that is very similar to the $I(V)$ characteristics of a two-ML silver film, albeit with an additional shoulder at approximately 7.5 eV, whose occurrence is described in the following paragraph. Here, we note that the qualitative match to the two-ML $I(V)$ curve suggests that additional silver atoms have adsorbed onto the one-ML film, finally creating small bilayer patches of silver. Since the shutter of the evaporator remained closed throughout the oxidation experiment, the additional silver has to originate from the sample surface itself. Consequently, Ag must have diffused from other regions of the surface to the ML islands.

Further insight into the Ag relocation process can be obtained from a detailed analysis of the local $I(V)$ spectra. For this purpose, we quote findings from a separate work [16], in which we analyzed the oxidation of the bare Ni(111) surface and its $I(V)$ behavior in a joint experimental and theoretical investigation. We found that an ultrathin NiO(111) film shows a sharp resonance at about 7.5 eV in the $I(V)$ spectra, whereas the reflectivity of the oxide layer remains rather low as compared with a Ag/Ni system. For reference, this NiO fingerprint is also reproduced along with the high-resolution $I(V)$ curve shown in Figure 2(a). As mentioned in the preceding paragraph, the same resonance can be also found as a shoulder after the one-ML silver film has been exposed to 285 L of oxygen. The most likely explanation for the $I(V)$ spectrum obtained after oxidation is to interpret it as the sum of the individual reflectivity values of the Ag/Ni(111) and NiO/Ni(111) regions. (Note that all attempts to simulate the $I(V)$ curve by the dynamic LEED theory within a structural model, including an oxygen adlayer on top or below a Ag film on the Ni(111) substrate, had to be discarded due to insufficient matching to the experimental data.) Further justification for this model is provided in a later section when we discuss our findings for oxidation at 600 K.

Structurally, the finding of an addition of single-phase $I(V)$ spectra implies that oxygen adsorption induces the formation of NiO domains, although the surface was originally covered by a silver film. In the course of the reaction of oxygen with nickel, silver atoms are liberated from this one-ML film, which subsequently attach to highly coordinated sites at oxygen-free Ag/Ni regions, creating small silver patches next to simultaneously growing NiO(111) regions. These silver patches form since epitaxial growth of silver on the NiO(111) surface is expected to be energetically unfavorable from well-known basic thermodynamic considerations in heteroepitaxy [17]: Because NiO grows in a layer-by-layer mode on silver surfaces [18], a layer-by-layer growth mode, and hence a layered structure of Ag on top of NiO, is not plausible. Apparently, the formation of silver patches and NiO regions

occurs at a very close range, i.e., on a lateral length scale that is small in comparison with the image resolution. Similar observations can be obtained for the two-ML silver film. Upon oxidation, the resonance at 7.5 eV starts to grow, whereas the main feature of the silver bilayer at 5 eV, which is a manifestation of the layer-dependent quantum size effect, disappears. This observation is compatible with the concomitant formation of even thicker silver patches and silver-free NiO(111) regions in an Ostwald-like ripening process.

The preferred oxidation of Ni as compared with Ag can be explained by both kinetic and thermodynamic arguments: In the investigated temperature range, Ni(111) exhibits a dissociative sticking coefficient that is about four orders of magnitude higher than for bulk Ag(111), rendering oxygen adsorption and dissociation on exposed nickel areas or defects much more favorable. Furthermore, the large difference in the individual energy gain values related to Ag–O and Ni–O bond formation is illustrated by the corresponding enthalpies H of formation of bulk silver oxide ($\Delta H_{F,Ag_2O} = -30.6\ \mathrm{kJ \cdot mol^{-1}}$ [19]) and bulk nickel oxide on the nickel surface ($\Delta H_{F,NiO} = -239.9\ \mathrm{kJ \cdot mol^{-1}}$ [20]) at room temperature.

The high-resolution $I(V)$ spectra of both one- and two-ML silver oxidation qualitatively show the same behavior. The only difference occurs with respect to the NiO peak intensity, which is higher in the case of oxidation of the one-ML silver film. In the sense of an incoherent superposition of the signals originating from NiO and Ag/Ni regions, the surface fraction, which is covered by NiO, is thus expected to be larger for the one-ML region than that for the two-ML region. Since the thermodynamic driving force for the dewetting process should be determined by the interaction between the developing oxide and the disintegrating silver film at the interface, it should be similar for both one- and two-ML-thick films. Because of the chemical inertness of silver, oxidation below the Ag film is predominantly initiated by oxygen transport via steps and domain boundaries between the Ag domains. However, the silver film thickness is also expected to have a considerable effect on the amount of exposed Ni defects, which provide natural points of attack for oxygen adsorption and subsequent oxidation. The finding of higher stability of the two-ML film thus suggests a more effective passivation of the nickel substrate and a lower number of reactive defect sites.

For the elevated temperature of 600 K, oxidation shows a similar behavior as the experiment performed at 500 K. Based on the local $I(V)$ curves, the bright regions [see Figures 2(b) and 3] can be identified as two-ML-thick silver islands, which have significantly grown upon *oxidation*. As already assumed for oxidation at 500 K, the most likely origin of the relocated silver atoms are the Ag ML film and the apparently bare Ni regions, where a substantial amount of silver adatoms is known to exist after the preparation [4]. Considering the changes in the $I(V)$ spectra for both regions, a possible scenario for the reaction with oxygen is the following: In the lattice gas regions, the oxygen atoms form an oxide on Ni(111) that destabilizes the silver atoms, which then diffuse over the surface by thermal activation. As a consequence, the residual silver atoms adsorb and finally agglomerate at highly coordinated step-edge sites of the second silver ML and thereby promote the growth of the silver bilayer regions. This effect is significantly enhanced by sequential Ag migration from the ML-thick large islands, which upon subsurface oxygen incorporation disintegrate to form silver-free areas in between that are finally transformed to NiO(111). As compared with oxidation at 500 K, the lateral size of the forming silver islands is larger for the 600-K oxidation, which we attribute to the higher mobility of the silver atoms due to enhanced thermal diffusion at higher temperature.

Finally, we investigated the effect of ethylene, a common reducing agent, on the atomic structure and morphology of the oxidized Ag/Ni system, which may constitute the second part of a chemical redox reaction at the surface of a silver–nickel model catalyst [21]. Under near-UHV conditions and at a substrate temperature of 600 K, the largest part of the silver-covered surface remains unaffected by the ethylene dose (see points "A" and "B" in **Figure 4**), which most likely points toward a relatively low reaction rate for NiO reduction by ethylene at this temperature. However, in some regions of the silver film, a small dose of ethylene already causes a change in contrast (see Figure 4). To clarify the origin of this change in reflectivity, we again monitored the evolution of the surface with dynamic LEEM-$I(V)$. After dosing of 420 L at 600 K, ethylene apparently initiates the decomposition of the second silver layer in some small regions (marked by orange lines), which is clearly corroborated by the corresponding local $I(V)$ curves recorded, e.g., at point "C." This observation can be interpreted in the following way: Oxygen is removed from smaller and larger NiO patches (see, e.g., point "D" in Figure 4, which previously constituted a mostly "bare" Ni region not covered by a dense silver layer before oxidation), where the nickel oxide peak at 7.5 eV significantly decreases upon ethylene dosage, inducing the presence of reactive Ag-free areas concurrent with a significant change in surface chemical potential. Hence, bilayer silver islands act as local sources of Ag and subsequently disintegrate (e.g., point "C" in Figure 4), establishing a substantial local Ag concentration in these surface regions. This transfer of Ag will most probably be accompanied by the formation of a lattice gas followed by ML island nucleation after supersaturation [4]. Considered together, these observations, in essence, demonstrate at least partial reversibility of the silver migration process in the redox reaction.

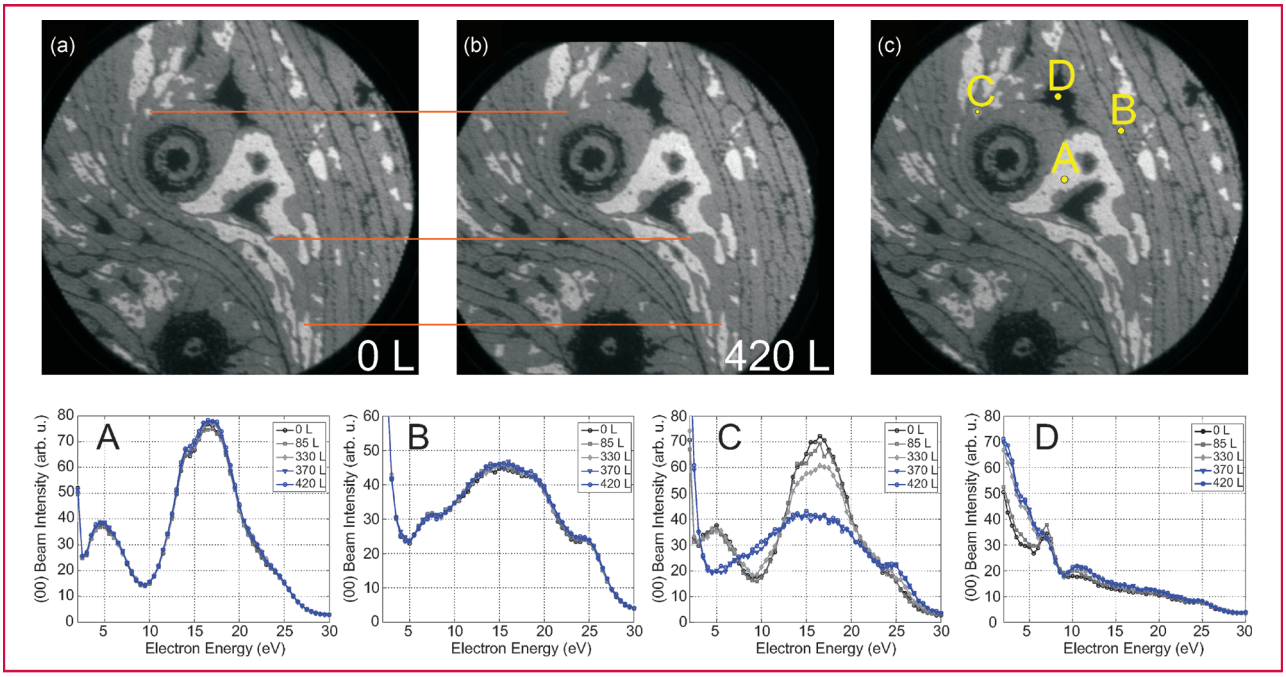

Figure 4

LEEM images of the surface (a) before and (b) after reduction of the oxidized surface with 420-L ethylene at a 10-μm field of view. The orange lines in (a) and (b) exemplarily show the regions where the ethylene changes the surface. The four sets of $I(V)$ curves have been taken at the points marked in (c).

Conclusion

We have presented an oxidation study of ultrathin silver films on the Ni(111) surface at 500 and 600 K. We found that exposure to oxygen at 500 K induces Ag migration processes that lead to the formation of a tight network of Ag patches and NiO regions. The same effect of Ag layer thickening has been found for oxidation at 600 K, albeit at a larger length scale, which is attributed to the higher mobility of silver atoms at higher temperature. A subsequent dose of ethylene onto the surface oxidized at 600 K causes oxygen removal from the Ni surface, whereas the two-ML silver islands shrink and dissolve, rendering the oxidation-induced migration process at least partly reversible. Therefore, we expect our results to also have profound consequences for the understanding of Ag/Ni and similar bimetallic systems in, for example, catalytic applications under reaction conditions.

Acknowledgments

The authors would like to thank Jurek Sadowski, Percy Zahl, Peter Sutter [Center for Functional Nanomaterials, Brookhaven National Laboratory (BNL)], and Gary Nintzel [National Synchrotron Light Source (NSLS), BNL] for technical support. This work was carried out at the Center for Functional Nanomaterials and NSLS, BNL, which are supported by the U.S. Department of Energy, Office of Basic Energy Sciences, under Contract DE-AC02-98CH10886.

References

1. B. Hammer and J. K. Nrskov, "Why gold is the noblest of all the metals," *Nature*, vol. 376, no. 6537, pp. 238–240, Jul. 1995.
2. B. Hammer and J. K. Nørskov, "Electronic factors determining the reactivity of metal surfaces," *Surf. Sci.*, vol. 343, no. 3, pp. 211–220, Dec. 1995.
3. X. J. Liu, F. Gao, C. P. Wang, and K. Ishida, "Thermodynamic assessments of the Ag–Ni binary and Ag–Cu–Ni ternary systems," *J. Electron. Mater.*, vol. 37, no. 2, pp. 210–217, Feb. 2008.
4. A. Meyer, J. I. Flege, R. E. Rettew, S. D. Senanayake, T. Schmidt, F. M. Alamgir, and J. Falta, "Ultrathin silver films on Ni(111)," *Phys. Rev. B*, vol. 82, no. 8, pp. 085424-1–085424-9, Aug. 2010.
5. A. Varykhalov, A. M. Shikin, W. Gudat, P. Moras, C. Grazioli, C. Carbone, and O. Rader, "Probing the ground state electronic structure of a correlated electron system by quantum well states: Ag/Ni(111)," *Phys. Rev. Lett.*, vol. 95, no. 24, pp. 247601-1–247601-4, Dec. 2005.
6. G. Rovida, F. Pratesi, M. Maglietta, and E. Ferroni, "Chemisorption of oxygen on the silver (111) surface," *Surf. Sci.*, vol. 43, no. 1, pp. 230–256, May 1974.
7. M. Schmid, A. Reicho, A. Stierle, I. Costina, J. Klikovits, P. Kostelnik, O. Dubay, G. Kresse, J. Gustafson, E. Lundgren, J. N. Andersen, H. Dosch, and P. Varga, "Structure of Ag(111)-p(4× 4)-O: No silver oxide," *Phys. Rev. Lett.*, vol. 96, no. 14, pp. 146102-1–146102-4, Apr. 2006.
8. C. T. Campbell, "Atomic and molecular oxygen adsorption on Ag(111)," *Surf. Sci.*, vol. 157, no. 1, pp. 43–60, Jul. 1985.
9. A. R. Kortan and R. L. Park, "Phase diagram of oxygen chemisorbed on nickel (111)," *Phys. Rev. B*, vol. 23, no. 12, pp. 6340–6347, Jun. 1981.
10. T. Okazawa, T. Nishizawa, T. Nishimura, and Y. Kido, "Oxidation kinetics for Ni(111) and the structure of the oxide layers," *Phys. Rev. B*, vol. 75, no. 3, pp. 033413-1–033413-4, Jan. 2007.

11. P. H. Holloway and J. B. Hudson, "Kinetics of the reaction of oxygen with clean nickel single crystal surfaces: II. Ni(111) surface," *Surf. Sci.*, vol. 43, no. 1, pp. 141–149, May 1974.
12. J. I. Flege, J. Hrbek, and P. Sutter, "Structural imaging of surface oxidation and oxidation catalysis on Ru(0001)," *Phys. Rev. B*, vol. 78, no. 16, pp. 165407-1–165407-5, Oct. 2008.
13. J. I. Flege and P. Sutter, "*In situ* structural imaging of CO oxidation catalysis on oxidized Rh(111)," *Phys. Rev. B*, vol. 78, no. 15, pp. 153 402-1–153 402-3, Oct. 2008.
14. J. I. Flege, E. Vescovo, G. Nintzel, L. H. Lewis, S. Hulbert, and P. Sutter, "A new soft X-ray photoemission microscopy beamline at the National Synchrotron Light Source," *Nucl. Instrum. Methods Phys. Res. B*, vol. 261, no. 1/2, pp. 855–858, Apr. 2007.
15. C. Chambon, J. Creuze, A. Coati, M. Sauvage-Simkin, and Y. Garreau, "Tilted and nontilted Ag overlayer on a Ni(111) substrate: Structure and energetics," *Phys. Rev. B*, vol. 79, no. 12, pp. 125412-1–125412-9, Mar. 2009.
16. J. I. Flege, A. Meyer, J. Falta, and E. E. Krasovskii. (2011). Self-limited oxide formation in Ni(111) oxidation. *Phys. Rev. B.*. Available: http://arxiv.org/abs/1104.3481
17. M. Copel, M. C. Reuter, E. Kaxiras, and R. M. Tromp, "Surfactants in epitaxial growth," *Phys. Rev. Lett.*, vol. 63, no. 6, pp. 632–635, Aug. 1989.
18. T. Bertrams and H. Neddermeyer, "Growth of NiO(100) layers on Ag(100): Characterization by scanning tunneling microscopy," *J. Vac. Sci. Technol. B*, vol. 14, no. 2, pp. 1141–1144, Mar. 1996.
19. J. Assal, B. Hallstedt, and L. Gauckler, "Thermodynamic assessment of the silver–oxygen system," *J. Amer. Ceram. Soc.*, vol. 80, no. 12, pp. 3054–3060, Dec. 1997.
20. B. J. Boyle, E. G. King, and K. C. Conway, "Heats of formation of nickel and cobalt oxides (NiO and CoO) of combustion calorimetry," *J. Amer. Chem. Soc.*, vol. 76, no. 14, pp. 3835–3837, Jul. 1954.
21. R. E. Rettew, A. Meyer, S. D. Senanayake, T.-L. Chen, C. Petersburg, J. I. Flege, J. Falta, and F. M. Alamgir, "Interactions of oxygen and ethylene with submonolayer Ag films supported on Ni(111)," *Phys. Chem. Chem. Phys.*, vol. 13, pp. 11 034–11 044, 2011.

Received October 1, 2010; accepted for publication February 16, 2011

Axel Meyer *Institute of Solid State Physics, University of Bremen, 28359 Bremen, Germany (meyer@ifp.uni-bremen.de).*

J. Ingo Flege *Institute of Solid State Physics, University of Bremen, 28359 Bremen, Germany (flege@ifp.uni-bremen.de).*

Sanjaya D. Senanayake *Chemistry Department, Brookhaven National Laboratory, Upton, NY 11973 USA (ssenanay@bnl.gov).*

Björn Kaemena *Institute of Solid State Physics, University of Bremen, 28359 Bremen, Germany (bkaemena@ifp.uni-bremen.de).*

Robert E. Rettew *School of Materials Science and Engineering, Georgia Institute of Technology, Atlanta, GA 30332 USA (r-rettew@gatech.edu).*

Faisal M. Alamgir *School of Materials Science and Engineering, Georgia Institute of Technology, Atlanta, GA 30332 USA (faisal.alamgir@mse.gatech.edu).*

Jens Falta *Institute of Solid State Physics, University of Bremen, 28359 Bremen, Germany (falta@ifp.uni-bremen.de).*